PPPL-3225, Preprint: January 1997, UC-420, 426

INVESTIGATION OF THE EFFECT OF RESISTIVE MHD MODES ON SPHERICAL TORUS PERFORMANCE IN CDX-U

M. ONO, D. STUTMAN, Y.S. HWANG[1], W. CHOE, J. MENARD, T. JONES, E. LO, R. ARMSTRONG[2], M. FINKENTHAL[3], V. GUSEV[4], S. JARDIN, R. KAITA, J. MANICKAM, T. MUNSAT, R. NAZIKIAN, Y. PETROV[4]

Plasma Physics Laboratory, Princeton University, Princeton, 08543, NJ, USA,

[1]Korean Advanced Institute for Science and Technology, Korea

[2]University of Tromsø, Tromsø, Norway.

[3] Johns Hopkins University, Baltimore, Maryland 21218, USA.

[4] Ioffe Institute, St. Petersburg, Russia.

DISCLAIMER

Portions of this document may be illegible in electronic image products. Images are produced from the best available original document.

INVESTIGATION OF THE EFFECT OF RESISTIVE MHD MODES ON SPHERICAL TORUS PERFORMANCE IN CDX-U

ABSTRACT - Resistive MHD modes and associated effects on spherical torus performance are investigated in the CDX-U device for $Ip \leq 100$ kA. Presently, the growth of resistive MHD modes (n=1/m=3 or n=1/m=2) as the edge q [q(a)] is lowered toward 3.5 appears to limit the maximum current achievable in CDX-U. For low q(a) discharges, a prominent rotating "hot" spot can be seen with the soft x-ray array, indicative of a magnetic island associated with a n=1/m=1 mode. The edge mode, which is n=1/m=3 or n=1/m=2, can be seen by the soft x-ray and edge magnetic pick up coil array. The growth of those modes in space and amplitude eventually leads to an Internal Reconnection Event (IRE). Prior to the IRE, strong mode-mixing takes place suggesting magnetic island overlap. The IRE causes a rapid heat loss from the core causing a strong plasma elongation and current spike due to the plasma inductance drop. With an appropriate discharge control, a MHD quiescent high confinement regime with over twice the central electron temperature relative to the MHD active regime has been found. To assess the halo-induced effects during the MHD events, a pair of segmented Rogowski coils were installed on the center stack. The observed halo-induced current fraction is generally small (less than 5 % of the total plasma current) even for the case of forced disruption.

1. INTRODUCTION

The spherical torus (ST) offers a promising possibility for a cost-effective high-performance plasma regime which could lead to a compact volumetric neutron source as well as an attractive economical power reactor [1]. Recent results from ideal MHD calculations are indeed encouraging, as MHD stable plasmas in excess of 45% beta, with ≥ 80% bootstrap (pressure driven) fraction and natural elongation of $\kappa \approx 2$, have been predicted[2,3]. With increasing elongation ($\kappa \approx 3$), a regime with 45% beta and nearly 100% bootstrap fraction (fully aligned bootstrap current regime) appears to be possible. On the experimental front, START reported very encouraging results on plasma confinement and the lack of plasma disruptions [5]. Similar observations in CDX-U have been reported [6]. While these experimental and theoretical results are very encouraging thus far, there are important issues regarding resistive MHD which deserve careful investigation. In START, a resistive MHD event, termed the IRE (the internal reconnection event), has been frequently observed. While the IRE does not terminate the plasma (like the hard disruption in a conventional tokamak), it still causes a relatively rapid heat loss from the plasma core. Resistive MHD instabilities, if not controlled, can also limit the ultimate operational parameters of spherical torus plasmas. It is therefore important to clarify the possible effects of resistive MHD modes on spherical torus performance, particularly in view of the next step ST experiments under construction (e.g., NSTX[4]). Recent ST design activity revealed a potential structural problem for high current STs if a significant fraction of plasma current (40%) is induced in the center stack, as is observed in many higher aspect ratio tokamak experiments. To assess the extent of halo-induced current in ST, halo related physics needs to be investigated particularly during strong MHD events such as IRE and disruption.

2. CDX-U EXPERIMENTAL SET-UP

The CDX-U torus is a spherical torus facility with $R \approx 32$ cm, aspect ratio $A \equiv R/a \geq 1.4$, and $B_{TF} \approx 1$ kG. Presently, an OH power supply with 60 m V-S capability is operational on CDX-U. The experiment was conducted up to $I_p \approx 100$ kA and $q(a) \geq 3.5$. Diagnostics include a 2-D scanning microwave interferometer, 30-element poloidal magnetic pick-up coil and toroidal coil arrays, Rogowski coils for plasma and wall eddy currents, a Mach probe, a 2-D scannable magnetic probe, soft x-ray and spectroscopic detectors, a multi-pass Thomson scattering system, and a tangential phase-contrast imaging system. New additions to the CDX-U diagnostics are the 19 channel soft x-ray array for the resistive MHD study and a pair of segmented Rogowski coils around the center-stack to measure the halo-induced currents flowing in the center-stack. The cross sectional view of CDX-U with magnetic and soft x-ray diagnostics are shown in Fig. 1 (a).

SOFT X-RAY DIODE ARRAY FOR MHD STUDY - As shown in Fig. 1, the 16 channel vertical soft x-ray array detects soft x-ray signal for various chordal vertical positions. Instead of the soft X-ray continuum above 1 keV used for MHD monitoring in large fusion devices, the CDX-U diode array uses the line emission of C V (He-like) and C VI (H-like) around 300 and 380 eV, respectively. This is much brighter than continuum emission, and in addition, in the temperature range up to a few hundred eV, these high ionization potential ions sample most of the plasma volume. To separate the high energy (soft X-ray) C line emission from intense emission of lower charge states (e.g. of O V, O VI at about 50-70 eV), we use the M-shell transmission band of very thin (0.2 micron), free standing Ag and Pd foils. The channel separation is 2.54 cm, and the spatial resolution at mid-plane is also ~ 2.5 cm with a total height of ~ 43 cm ($Z = \pm 21.5$ cm). An additional channel filtered for low energy (O V, O VI) emission is used at the top ($Z = +24$ cm) to monitor emission closer to the edge. Thus, the plasma is sampled on a regularly spaced grid, which is a major simplification in the data interpretation, especially when dealing with a highly shaped plasma as in CDX-U. The detector system has 10 μsec fast time resolution, and therefore, it is a very effective tool for MHD activity observation.

3. PLASMA CURRENT LIMIT AND RESISTIVE MHD MODES

Since ST reactor performance depends strongly on the amount of plasma current which can be supported, it is important to explore this current limit of STs. Experimentally, the current limit in CDX-U is reached when the plasma edge safety factor q reaches about 3.5. Figure 1(b) shows the plasma current values obtained in

CDX-U as a function of applied toroidal field strength, and suggests that the plasma current limit is generally proportional to toroidal field.[2-3] With a modest change (≈ 5%) of plasma aspect ratio and elongation, the allowable current limit for q(a) = 3.5 can be substantially (≈ 40%) increased as shown by the dashed curve. Significantly higher plasma current (≈ 30%) was indeed obtained (crosses versus circles). The minimum q(a) value appears to be limited by resistive MHD instability. Studies of magnetic fluctuations revealed an increasing activity of coherent resistive MHD oscillations as the q(a) is lowered. Temporal and spatial characteristics of the dominant oscillations were measured by poloidal and toroidal magnetic pick-up coil array, soft x-ray array, and phase-contrast diagnostics. Coincident with this current limit, we observe the rapid growth of an n=1, m=3 mode (or the 1/3 mode) [8], and more recently n=1, m=2 (or the 1/2 mode) for higher current cases. While the 1/3 and/or 1/2 modes do not cause a hard disruption, the increased MHD activity makes it difficult to raise the plasma current, imposing a practical limit for the achievable current as shown in Fig. 1(a). In a spherical torus configuration, due to a rapid change in the q value near the edge region, the q=3/q=2 layers are located relatively close to the plasma edge even when q(a) value is significantly larger than 3.

4. RESISTIVE MHD MODES AND INTERNAL RECONNECTION EVENTS IN CDX-U

The dominant resistive MHD modes observed thus far are mainly n=1 and m=1, 2, 3. There are several mode of operation which can significant change the resistive MHD mode behavior. In Fig. 2, we show soft x-ray [(a) and (c)] and magnetic fluctuation signals [(b) and(d)] for two types of discharges, of which end with an IRE event. The y-axis is diode array position (from top to bottom) and magnetic pick-up coil position covering whole poloidal angle (top half is low field side and bottom half is high field side). To aid visualization, the signal amplitude for each soft x-ray diode array and magnetic pick up coil array is indicated by the shades (i.e., darker for larger amplitude). Figure 2 (a) shows the soft x-ray "hot" spot (n=1/m=1) rotating in time with frequency of ≈ 8-9 kHz. It should be noted that the size of n=1/m=1 mode (which is also related to the q=1 layer) is quite large, $\Delta Z \approx 25$cm (reflecting the fact $q_{cyl} \approx 1.$). The edge channel shown in the top of Fig. 2(a) also shows an increased activity toward IRE. Similar observation can be seen in the magnetic pick up coil array as shown in Fig. 2 (b). Here, the dominant mode at the edge appears to be n=1 and m=2. It is interesting to note the low field side signals are quite coherent but the high field side signals are complicated with the presence of higher harmonic components. The same frequency for both dominant n=1 modes (m=1 and m=2) indicate that the plasma is rotating toroidally as a rigid body (with speed of nearly 30 km/sec at the outer plasma edge.). As shown in Fig. 2, both internal and external modes grow in size and amplitude while the plasma rotation slows down by 10-20% until the Internal Reconnection Event (IRE) occurs. This observation indicates that the mode-coupling or islands overlap is triggering the IRE event. We note here that the phase-contrast-imaging diagnostic also detects similar core MHD fluctuation signals with a radial coherence length consistent with the soft x-ray array result. Figure 2(c) and (d) shows a case which starts with a sawtoothing behavior with relatively quiet edge. However, later in the discharge, coherent modes appear and the discharge evolves into an IRE in a similar manner as the first case. As can be seen in the soft x-ray signal, during the IRE, the heat is transported rapidly from the core to the outer region. When the IRE occurs, due to decreasing core temperature, the current profile relaxes and the plasma inductance drops. This causes a spike-like increase in the plasma current while the plasma naturally elongates due to the decreased plasma internal inductance. It is interesting to note that even with IRE, the plasma is still quite resilient, and we observed that the central core rapidly reheats after the event.

MHD QUIESCENT DISCHARGES - While an IRE does not lead to a hard disruption, it is quite clear that we would like to avoid it if at all possible. Interestingly, we find that if we program our discharge appropriately, we can indeed obtain MHD-quiescent, IRE-free discharges. In Fig. 3(a) and (b), the time evolution of two MHD distinct discharges is shown. The first discharge [Fig. 3(a)] has usual MHD behavior similar to the one shown in Fig. 2. The second discharge, with a slightly different current ramp-up rate [Fig. 3(b)], is relatively free of the MHD activity and IRE. The measured Thomson scattering central temperature for the MHD quiescent discharge is about 140 eV, which is more than twice that of the first case of 65 eV. It is worthwhile to note that the MHD quiescent discharge has a second current ramp up phase, which might give a broader current profile. Since the total plasma current and plasma density are similar for the two cases [i.e., same q(a)], the difference in the MHD behavior can be attributed to differences in the plasma current profiles. It is therefore encouraging that the MHD behavior can be controlled by the discharge programming, yielding a factor of 2 - 3 improvement in plasma confinement. In the higher temperature regime (140 eV), these discharges have very low collisionality, with ν^* below 0.1 in most of the plasma volume.

6. HALO-CURRENT STUDY IN CDX-U

MOTIVATION OF HALO-CURRENT STUDY FOR ST - When a tokamak plasma undergoes a strong MHD event such as a plasma disruption, a variety of currents can be induced on the vacuum vessel wall. The effects of halo-induced current were first observed in PBX-M [9] where it was found that these currents caused significant damages to the plasma facing components (PFC)[8]. Subsequent experiments and MHD simulations have shown that when the disrupting plasma touches two poloidal locations of vacuum vessel, due to the EMF drive of decaying plasma current, a significant poloidal current can flow between the contact points in the vacuum vessel wall [9,10]. The current path is completed by the so-called halo currents flowing in the plasma edge region. Moreover, since plasmas in the disruption phase often undergo violent non-axisymmetric movements, the observed halo currents are not uniform around the torus. The unbalanced halo-induced currents in the inner wall (high field side) of large scale tokamaks (with Ip ≈ 10s' of MA, B_{TF} ≈ 10T) are of particular concern due to high j_{halo} x B_{TF} forces on the inner vacuum vessel wall and PFCs (≈ 10^4tons/m/10T/10MA). Through many tokamak experiments, a reasonable upper limit of halo-induced wall current in the inner wall appears to be 40% of the total plasma current with toroidal peaking factor of 2 over the average value. For the future spherical torus device, this halo-induced current in the center-stack (the inner leg of TF) also presents a potentially serious structural problem. It is therefore important to understand the nature of halo currents in the spherical torus plasmas. To facilitate this study, a segmented (4-element) Rogowski coil was placed in the upper and lower areas of the center-stack (as shown in Fig.1), measuring the total poloidal current flowing in the center-stack as well as up-down and toroidal asymmetry. The Rogowski coils are calibrated with the known TF current.

HALO-CURRENTS DURING IRE AND FORCED DISRUPTION IN CDX-U - As mentioned above, during an IRE, the plasma experiences a relatively violent increase in plasma elongation and plasma current, due to decreased plasma inductance. A typical plasma current trace is shown in Fig.4 (a) during the time of IRE. While the IRE is not a hard disruption, the plasma clearly touches the top and bottom of the vessel due to increased elongation, as seen by a TV camera and limiter currents. The raw halo-induced Rogowski coil voltage is shown in Fig. 4 (b) and (c) for the top and bottom Rogowski coils. The current is obtained by integrating the signal and is typically less than 1% of the total plasma current for both top and bottom coils. It should be noted that the halo-induced current pulse is very short (50 μsec), and the toroidal asymmetry is approximately 2:1. During the normal course of CDX-U operation, the IRE is the most serious MHD event in terms of the induced halo current. Otherwise, the ST plasmas in CDX-U are remarkably stable and resilient. It is, however, possible to artificially cause a rapid termination by deliberately turning down the toroidal field such that the q-limit is reached before developing into a full spherical torus configuration. This type of situation might be envisioned for some failure mode which may occur during the operational life of a ST reactor. This type of termination is shown in Fig. 4 (d), (e), and (f). The integrated Rogowski signal indicates that the rapid termination (or disruption) can induce current in the center-stack of up to ≈ 5% of the plasma current value - which is still an order of magnitude lower compared to what has been observed in tokamaks to date. It appears that when the plasma suddenly loses equilibrium, the plasma tends to move up or down, but is not sufficiently compressed in major radius and forced to ride on the small radius inner wall of the ST. The ST plasma appears to be stable against tilt or shift instability as well. Perhaps largely due to this MHD stability and geometric factor, the halo-induced current in the center-stack may be relatively small during and IRE and/or accidental disruption for ST. While this is an encouraging result for future STs, it is important to understand the physical mechanism of halo current in the ST geometry through further experimentation and theory/modeling.

ACKNOWLEDGMENT
We thank Jim Taylor and John Robinson for their technical support. We also thank Drs. S. Kaye, R. Goldston, and M. Peng for helpful comments. Work is supported by DoE contract Nos. DE-AC02-76-CHO-3073 and DoE grant No. DE-FG02-86ER52314AT.

REFERENCES:

[1] Peng, Y.-K.M., et al., IAEA -CN-60/F-1-I-3-3.

[2] Menard, J., et al., Bull Am. Phys. Soc. 40, 1655 (1995).

[3] Miller, R.L., Chan, V. S., et al., Bull Am. Phys. Soc. 40, 1788 (1995).

[4] Ono, M., et al., Bull Am. Phys. Soc. 40, 1655 (1995).

[5] Sykes, A., et al., Plasma Physics and Controlled Fusion **35**, 1051 (1993).

[6] Hwang, Y.S., et al., Bull Am. Phys. Soc. 40, 1654 (1995).

[7] D. Stutman, J. Menard, W. Choe, et al., to be published in Rev. Sci. Instru, (Jan. 1997).

[8] Jones, T. G., Ph.D. Thesis, Princeton University, Nov. 1995.

[9] Kugel, H.W., et al., in Controlled Fusion and Plasma Physics(Proc. 16th Eur. Conf. Venice, 1989), Vol. 13B,Part I, European Physical Society, Geneva (1989) 199

[10] Sayer, R.O., Peng, Y.-K.M., Jardin, S.C., et al., Nuclear fusion, Vol. 33, No. 7 (1993).

FIGURE CAPTIONS

Fig. 1. CDX-U diagnostics and current operational limits. (a) Cross sectional view of CDX-U device with magnetic and soft x-ray diagnostics. (b) Ohmic plasma current versus toroidal magnetic field. The current limit of q(a) is shown for two different values of aspect ratio R/A and elongation κ.

Fig. 2. Temporal behavior MHD modes leading to IRE. (a) and (b) The soft x-ray array and magnetic pick-up coil array signals of MHD active discharge are displayed, respectively. The shade depicts the MHD amplitude darker being higher amplitude. (c) and (d) Similarly for a sawtoothing discharge which later evolves into the MHD active discharge.

Fig. 3 The temporal evolution of plasma current, line integrated density, and soft x-ray signal. (a) Discharge with MHD. (b) Discharge with relative MHD quiescence. I_p = 60 kA, B_T = 1 kG.

Fig. 4 Halo-Induced Current in Center-Stack. (a), (b), and (c) - The plasma current evolution, the top Rogowski coil signal trace, and the bottom Rogowski coil signal trace, respectively, during IRE. Similarly, (d), (e), and (f) during forced disruption.

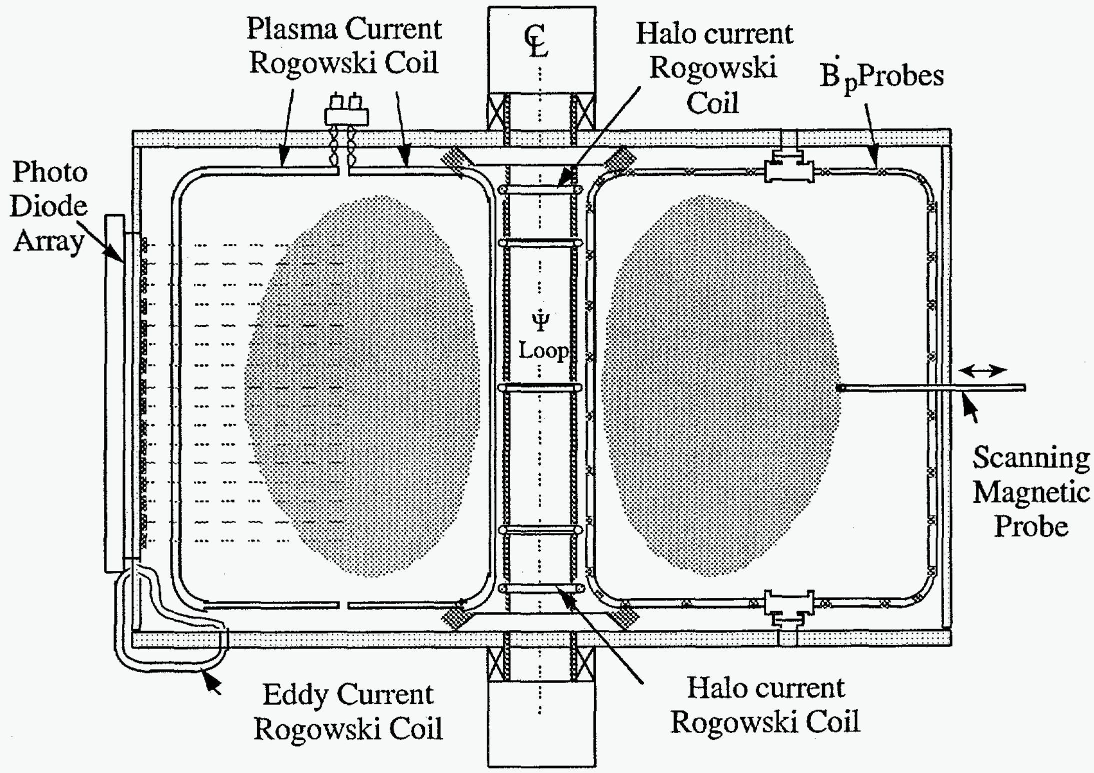
Plasma Current
Rogowski Coil
Halo current
Rogowski
Coil
$\dot{B}_p$Probes
Photo
Diode
Array
Ψ
Loop
Scanning
Magnetic
Probe
Eddy Current
Rogowski Coil
Halo current
Rogowski Coil

(b)

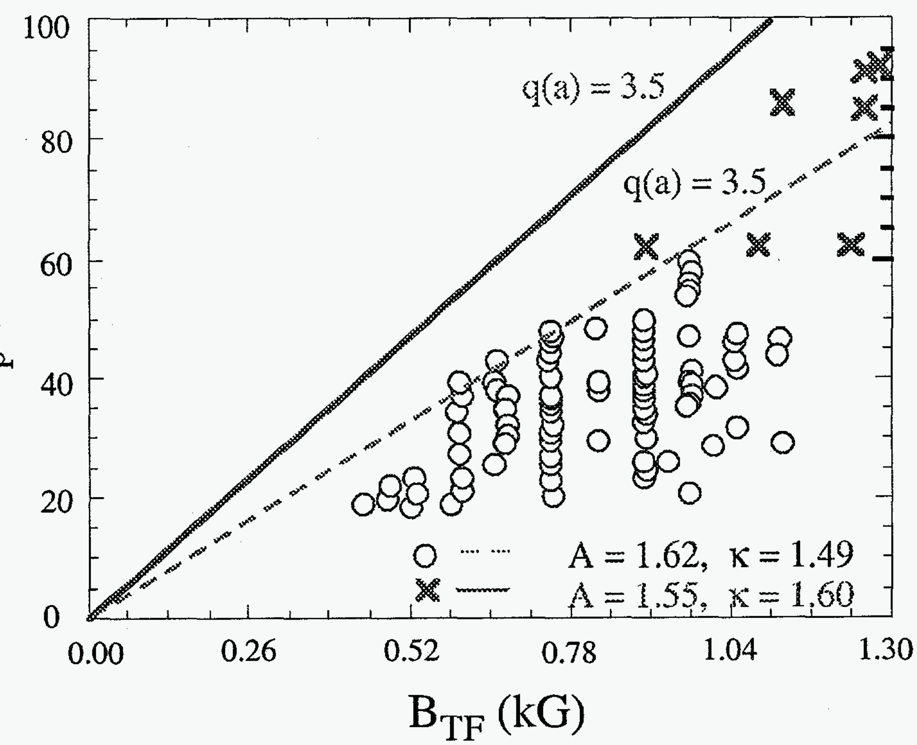
100
80
60
40
20
0
q(a) = 3.5
q(a) = 3.5
A = 1.62, κ = 1.49
A = 1.55, κ = 1.60
0.00
0.26
0.52
0.78
1.04
1.30
I_p (kA)
B_{TF} (kG)

Fig. 1

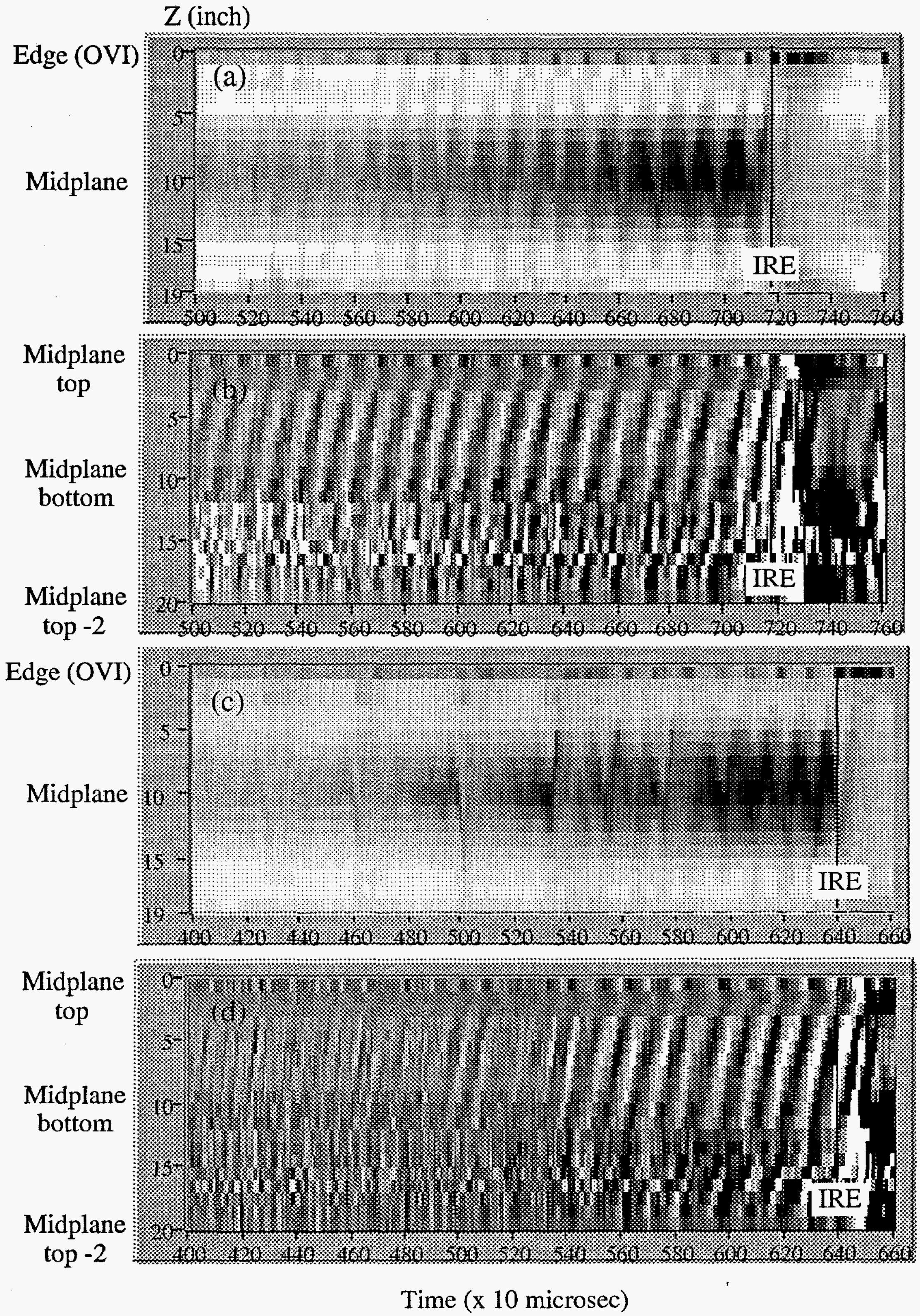

Z (inch)
Edge (OVI)
(a)
Midplane
IRE
0
5
10
15
19
500
520
540
560
580
600
620
640
660
680
700
720
740
760
Midplane top
(b)
Midplane bottom
Midplane top -2
IRE
0
5
10
15
20
Edge (OVI)
(c)
Midplane
IRE
400
420
440
460
480
500
520
540
560
580
600
620
640
660
Midplane top
(d)
Midplane bottom
Midplane top -2
IRE
Time (x 10 microsec)

Fig. 2

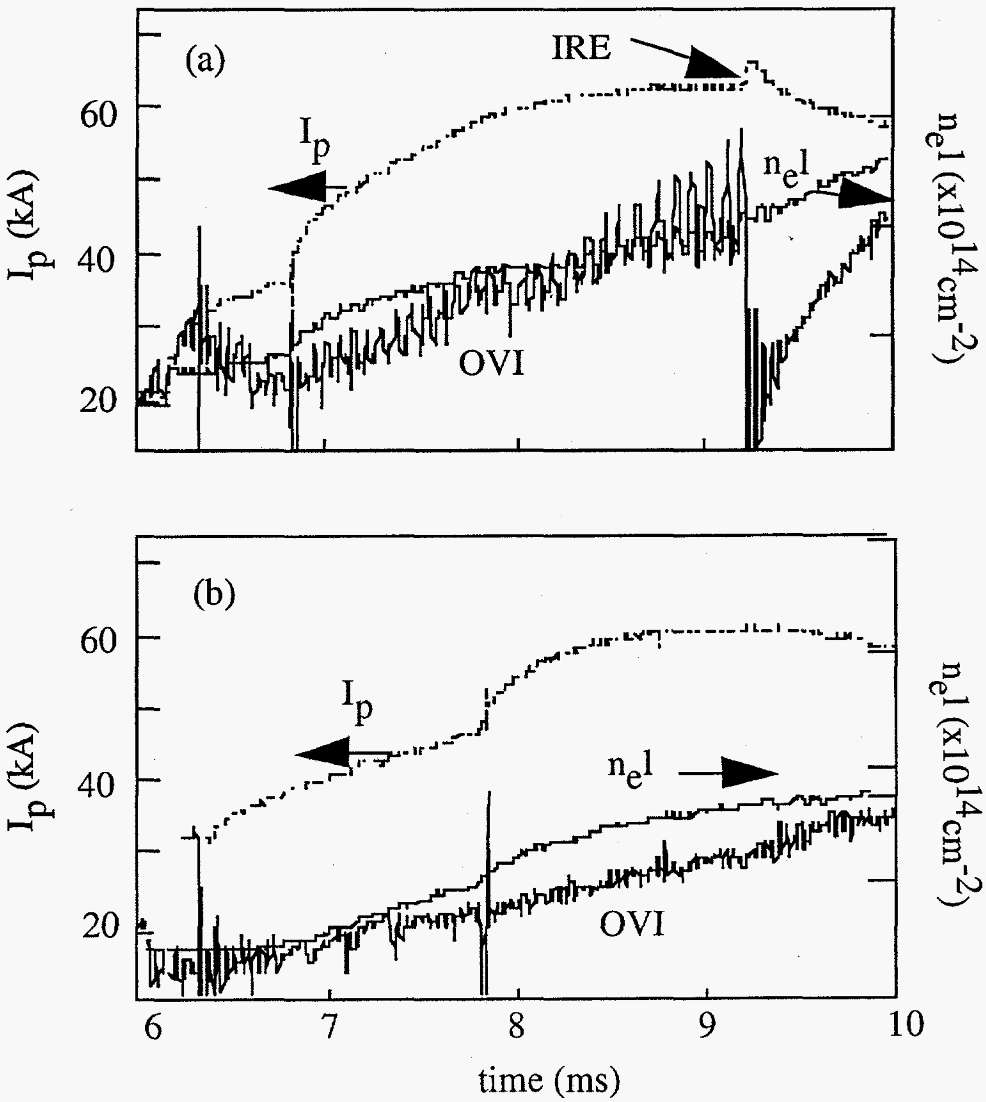
(a)
IRE
I_p
n_el
OVI
I_p (kA)
n_el (x10^{14}cm^{-2})
60
40
20
(b)
I_p
n_el
OVI
I_p (kA)
n_el (x10^{14}cm^{-2})
60
40
20
6
7
8
9
10
time (ms)

Fig. 3

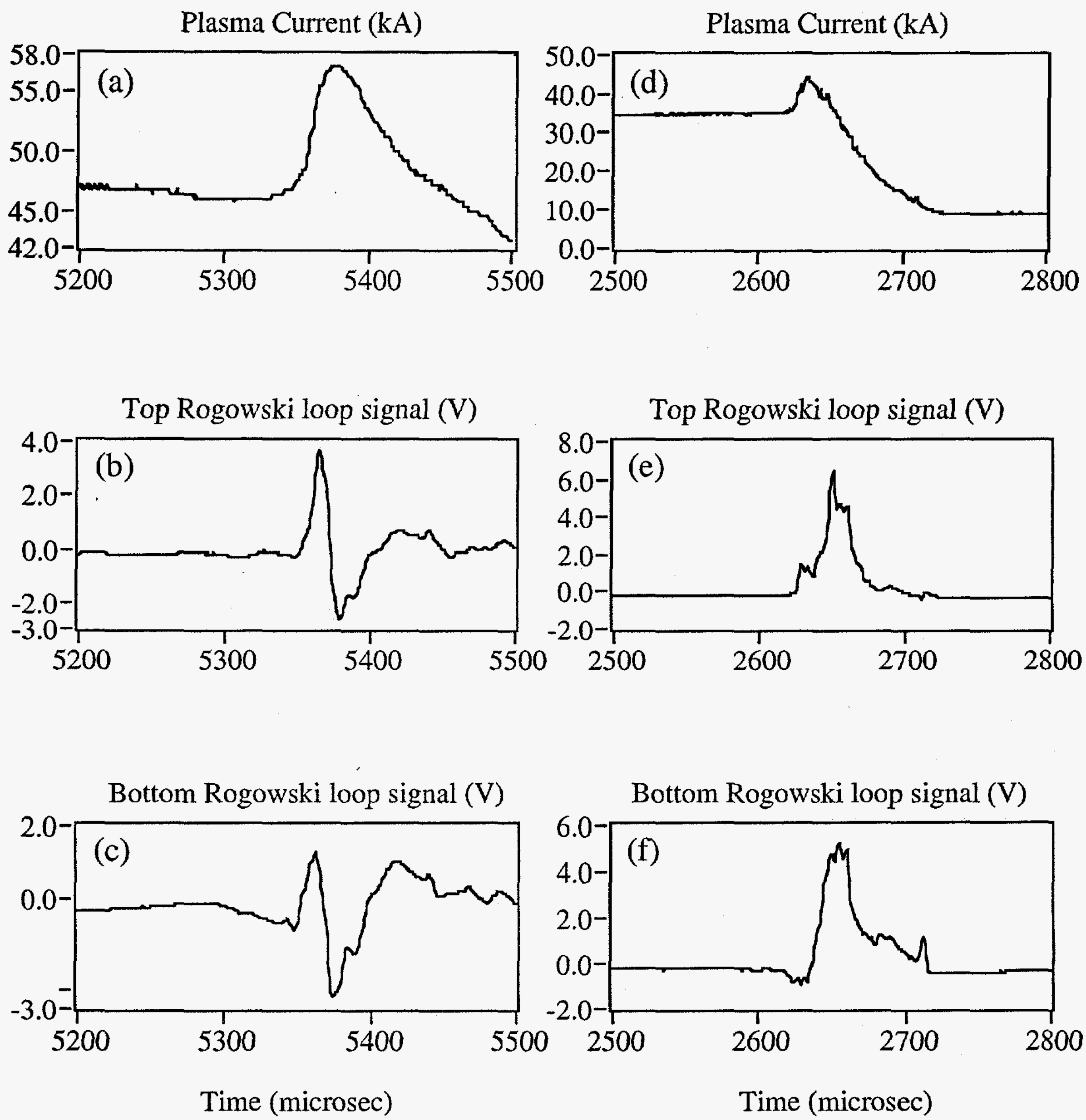
Plasma Current (kA)
58.0
55.0
50.0
45.0
42.0
(a)
5200
5300
5400
5500
Plasma Current (kA)
50.0
40.0
30.0
20.0
10.0
0.0
(d)
2500
2600
2700
2800
Top Rogowski loop signal (V)
4.0
2.0
0.0
-2.0
-3.0
(b)
5200
5300
5400
5500
Top Rogowski loop signal (V)
8.0
6.0
4.0
2.0
0.0
-2.0
(e)
2500
2600
2700
2800
Bottom Rogowski loop signal (V)
2.0
0.0
-3.0
(c)
5200
5300
5400
5500
Bottom Rogowski loop signal (V)
6.0
4.0
2.0
0.0
-2.0
(f)
2500
2600
2700
2800
Time (microsec)
Time (microsec)

Fig. 4